# SUSPENSION PLASMA SPRAYING OF HYDROXYAPATITE

**E. Bouyer, F. Gitzhofer and M.I. Boulos**

Plasma Technology Research Center (CRTP)
Department of Chemical Engineering, Université de Sherbrooke
Sherbrooke, Québec, Canada

## Abstract

We describe a new process of plasma deposition applied to bioceramic. Suspension Plasma Spraying (SPS) involves a ceramic colloidal suspension as the raw material for plasma spraying and takes full advantage of the inherent properties of the RF inductively coupled plasma (large volume, low gas velocity, electrode-less plasma torch). Coatings produced by SPS with a high deposition rate (>100μm/min) are well crystallized and show crystallographic texture according to (002) Miller's planes.

## 1. Introduction

Calcium phosphate ceramics are currently used for biomedical applications. Metal implants coated with bioactive calcium phosphate ceramics are very interesting in orthopedic and dental practice [1]. Hydroxyapatite - HA, $Ca_{10}(PO_4)_6(OH)_2$- used as a coating on titanium implants can bond to bone without bone resorption around it. Usually, such coatings are produced by thermal plasma spraying [2-3]. However, it has been pointed out that the dc plasma arc atmosphere is often contaminated with the electrode materials, tungsten and copper metals, carried from the electrode by erosion during the plasma operation. Radio frequency plasma technology possesses advantages over other techniques such as its relatively large volume and low velocity of the plasma gases which, when coupled with the ease of axial injection of the powder into the plasma allows for the melting of relatively large particles at high throughputs [4-5]. The absence of electrodes offers the added advantage of operations under a wide range of conditions at atmospheric and lower pressures and with an inert, reducing or oxidizing atmosphere. This present study is concerned with the production of HA coatings using a newly developed technique called Suspension Plasma Spraying (SPS) [6]. The process involves the injection of the HA material in

the form of an atomized colloidal suspension into the center of an inductively coupled Radio Frequency (RF) plasma discharge. This process involves powder-less (colloidal suspension) plasma spraying. The HA suspension is brought into the plasma discharge core by a gas atomizing probe. As the droplets are fed into the plasma they are flash dried and melted before being deposited on the substrate to be coated. The process takes full advantage of the inherent features of induction plasma discharge which allows sufficient time for the droplet drying and melting steps. Fig. 1 shows schematically the main three routes for HA deposit preparation. The SPS route is by far the simplest, least costly and eliminates many potentially contaminating steps.

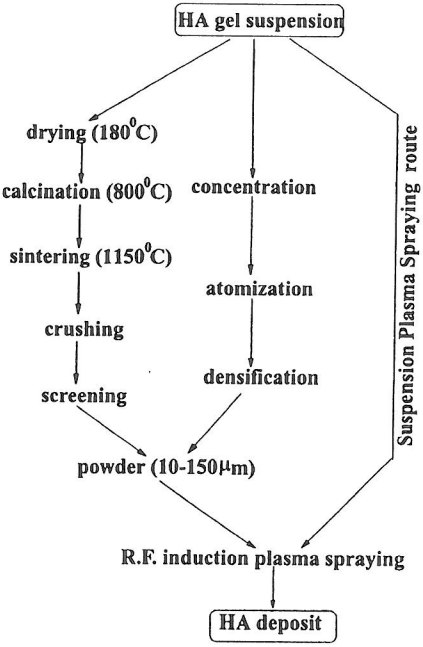


Figure 1 - Routes for HA coating preparation.

## 2. Experimental

An aqueous HA suspension containing around 40% wt solid is used as the process raw material. The HA synthesized is wet chemically synthesized in our laboratory following the method of Aoki *et al.* [7]. The precursors are $Ca(OH)_2$ and $H_3PO_4$. The resulting HA suspension is plasma sprayed using the installation of RF plasma spray deposition described by Boulos, [5], using the torch and atomizing probe as presented in Fig. 2. The HA suspension is fed via a peristaltic pump and is gas atomized directly into the RF plasma generated by the RF plasma torch, a 50 kW Tekna Plasma System Inc. PL50 model. Spray sample substrates used are both of stainless steel (316L) as plates (50x35x1.5 mm) and of graphite as disks (95 mm diameter). Before use in spraying stainless steel substrates were grit blasted with 40 grit alumina powder. Table 1 sets out the SPS process conditions employed. In this study, we present the influence of the reactor conditions on the HA coating properties. TEM investigations of the pre spray HA colloids were performed with a Philips EM 300G microscope. X-ray diffraction patterns were measured directly on the as-deposited coated plates using a RIGAKU D/max X-ray powder diffractometer. HA deposit morphological analyses were performed on a Jeol

JSM-840A scanning electronic microscope.

## 3. Results and discussion

Fig. 3 depicts a TEM picture of the HA particulates immeadiatly after wet chemical synthesis, the needle shape crystals (20x200 nm average) is characteristic of HA when synthesized at low temperature (42 $^0$C) and are derived from the hexagonal structure of HA. In order to study the melted state of the powder before it is impinged onto the substrate, in-flight SPS generated powder was collected into water, using same plasma conditions as indicated in table 1. Through examination of the SPS water collected droplets, their morphology, just before they impinge onto the substrate, is accessed. In Fig. 4 spherical atomized SPS droplets are displayed having a 15 μm average diameter. Two typical powder morphologies can be distinguished ; (a) spherical smooth particles with grain boundaries (not visible at this magnification) and (b) spherical powders with "pinholes". In Fig. 5, the fracture of a plasma sprayed HA coating, a relatively high density (>70% measured by the Archimedes method) with some spherical, included powder grains is shown. The surface of the coating as presented in Fig. 6 is tortuous. This surface morphology leads to the improvement of the anchorage between natural bone and SPS HA coatings [8].

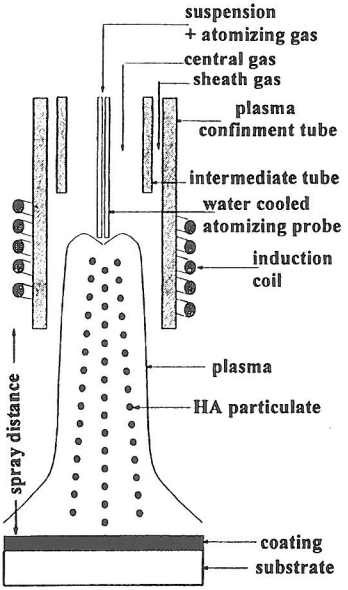


Figure 2 - Schematic RF torch and substrate.

X-ray diffraction analysis of the HA (dried) suspension shows broad peaks characteristic of the pure HA (Fig. 7a). On the other hand, HA coatings obtained by RF SPS show a crystallographic preferred orientation Fig. 7b. As identified by Kameyama *et al.* [9], this orientation is along the (002) Miller's plan. We defined an index of preferential orientation noted as $n_{P.O.}$ :

Table 1 - Plasma spraying conditions

| | |
|---|---|
| plasma gas (slpm) | |
| . central (Ar) | 45 |
| . sheath (Ar+$H_2$) | 85+5 |
| . carrier gas (Ar) | 5 |
| plate voltage (kV) | 7.0 |
| plate current (A) | 5.5 |
| power (kW) | 38.5 |
| spray distance (mm) | 220 |
| HA flow rate (g/min) | 5.0 |
| reactor pressure (kPa) | 30 - 70 |

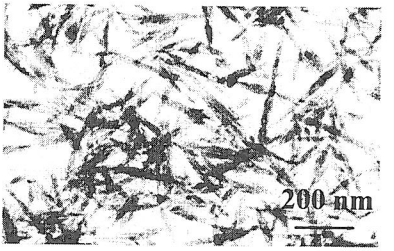


Figure 3 - TEM picture of HA colloids.

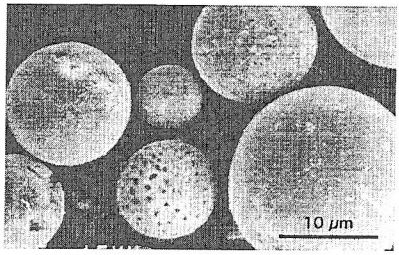


Figure 4 - HA SPS in water.

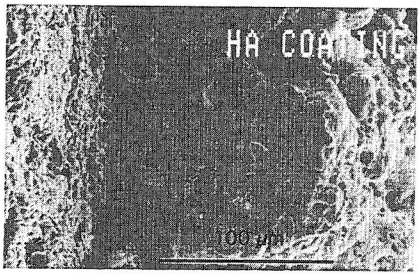


Figure 5 - HA SPS fracture.

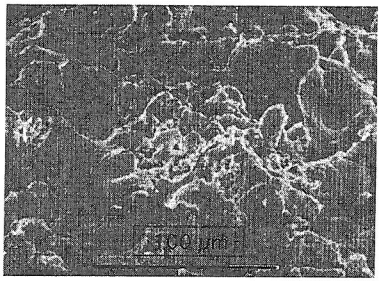


Figure 6 - HA SPS coating (top view).

$$n_{P.O.} = \frac{I^{C}_{(002)}}{I^{C}_{(211)}}$$

$I^{C}_{(002}$ represents the diffracted intensity (cps) of the (002) peak for the coating and $I^{C}_{(211}$ represents the diffracted intensity (cps) of the (211) peak for the coating. The (211) diffracted peak corresponds to the more intense peak. For HA spray powder (without crystallographic orientation) $n_{P.O.}$ should be equal to 0.4 (JCPDS #9-432). In all coatings obtained by SPS with the RF inductively coupled plasma, $n_{P.O.}$ reaches higher values than 0.4. In Fig. 8, the

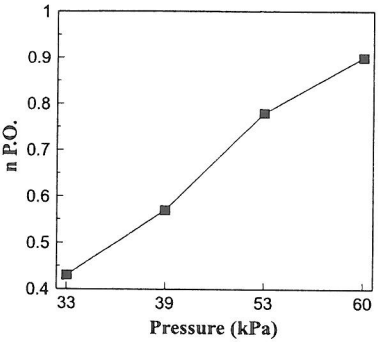


Figure 8 - Influence of the reactor pressure on $n_{P.O.}$ for HA SPS.

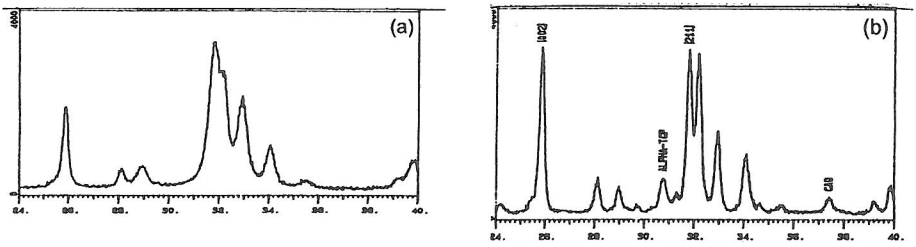


Figure 7 - (a) XRD pattern of as-synthezised HA ;
(b) XRD pattern of SPS HA coating.

variation of $n_{P.O.}$ of powders versus the reactor pressure during spray experiments shows that preferred orientation increases with the pressure. This behavior can be explained by multiple phenomena that closely interact : i.e. the atomization conditions which very interact with the chamber pressure, the heat transfer as well as mass transfer during water vaporization, the dry powder heat transfer up to the melting point which depends on plasma particle interactions and residence time, the substrate temperature which also depends on the pressure. The pressure parameter appears to have a high impact on the process and is still under study. From the material science view point the explanation for the crystallographic texture involving grain growth along the HA C-axis, which possesses a hexagonal structure (space group $P6_3/m$), is caused by the fact that the lowest surface energy plane of HA (i.e. the more stable thermodynamically) corresponds to the (00ℓ) Miller's plane family. This preferential orientation can also be observed in human bones and teeth enamel, it contributes to the high mechanical strength of these structures [10].
By means of XRD it is possible to detect a small degree of decomposition of the HA during the plasma heat treatment which can be described by the following decomposition reaction :

$$Ca_{10}(PO_4)_6(OH)_2 \rightarrow 3Ca_3(PO_4)_2 + CaO + H_2O$$

α-TCP is the high temperature equilibrium phase of tricalcium phosphate ($Ca_3(PO_4)_2$).

## 4. Conclusions

Suspension Plasma Spraying has been developed for HA coatings. This powder-less spraying technique involves colloid suspension atomized in a RF

induction plasma torch. In this paper, we have shown the feasibility of this technique for HA deposition with high deposition rates (>150 μm/min). This process takes full advantages of the features of RF plasma generation, i.e. its high residence time and plasma volume, and permits a crystallographic orientation in the deposit following the (002) Miller's planes because of the relatively good melting state attained during the plasma heat treatment. Moreover, the electrode-less plasma generation process leads to a high purity product without significant contamination which is a key requirement in the biomaterial field. In future work, we foresee the improvement of the HA injection into the plasma (i.e. atomization), and the implemention of *in vitro* tests of our HA deposit achieved by SPS - such as dissolution and/or phase transformation occurring in artificial physiological solution - and the testing of the mechanical adhesion of SPS HA deposits.

## Acknowledgment

This project was funded by the Natural Sciences and Engineering Research Council of Canada (NSERC). The authors are very gratefull to M. P. Magny for his technical assistance on the TEM and SEM work.

## References

1 Doremus, R. H., Journal of Material Science 27, 285-297 (1992).
2 Wolke, J. G. C., J. M. A. de Blieck-Hogervorst, W. J. A. Dhert, C. P. A. T. Klein and K. de Groot, Journal of Thermal Spray Technology 1, 75-82 (1992).
3 Berndt C. C., G. N. Haddad, A. J. D. Farmer and K.A. Gross, Materials Forum 14, 161-173 (1990).
4 Boulos M. I., Pure & Appl. Chem. 57, 1321-1352 (1985).
5 Boulos M. I., Journal of Thermal Spray Technology 1, 33-40 (1992).
6 Gitzhofer F., E. Bouyer and M.I. Boulos, U.S. patent n$^0$ 8,296,674 (1994).
7 Aoki H., M. Akao, Y. Shin, Y.Tsuzi and T. Togawa, Medical Progress through Technology, 12, 213-220 (1987).
8 Franck R.M. and E.P. Benque, in Proceeding of 26$^{ième}$ colloque de microscpie électronique, Nantes , France (1984).
9 Kameyama T., A. Hasegawa, A. Motoe, M. Ueda, K. Onuma, K. Akashi and K. Fukuoda, in Proceeding of Jpn. Symp. on Plasma Chem. 6, Tokyo, Japan (1993).
10 Abe Y., M. Osoe, T. Kasuga, H. Ishikawa, N. Shinkai, Y. Suzuki and N. Nakayama, Journal of American Ceramic Society 65, C-189 (1982).